Krishan *et al. Int J Concr Struct Mater* (2018) 12:84
https://doi.org/10.1186/s40069-018-0322-z

International Journal of Concrete Structures and Materials

RESEARCH Open Access

Strength Calculation of Short Concrete-filled Steel Tube Columns

Anatoly Leonidovich Krishan[1], Mariia Anatolyevna Astafeva[2] and Elvira Petrovna Chernyshova[3*]

Abstract

The aim of this work is to propose a technique to calculate the strength of short concrete-filled steel tube columns under the short-term action of a compressive load, based on the phenomenological approach and the theoretical positions of reinforced concrete mechanics. The main dependencies that allow the realization of the deformation calculation model in practice are considered. A distinctive feature of the proposed approach is the method of the multipoint construction of deformation diagrams for a concrete core and steel shell. In this case, two main factors are taken into account. First, the steel shell and the concrete core work under conditions of a complex stress state. Since the proposed dependencies to determine the strength and the ultimate relative strain of volumetrically compressed concrete are obtained phenomenologically, they are more versatile than the commonly used empirical formulas. In particular, they can be used for self-stressing, fine-grained and other types of concrete. Second, with a step-by-step increase in the relative deformation, the lateral pressure on a concrete core and a steel shell constantly change. Thus, the parametric points of the concrete and steel deformation diagrams also change at each step. This circumstance was not taken into account in earlier calculations. A comparison of the theoretical and experimental results indicates that the practical application of the developed calculation procedure gives a reliable and fairly stable estimate of the stress–strain state and the strength of concrete-filled steel tube columns.

Keywords: concrete-filled steel tube columns, strength calculation technique, deformation model, deformation diagram, concrete core, steel shell

1 Introduction

Concrete-filled steel tube columns (CFTC) are steel-reinforced concrete structures. The proposed methods for the calculation of a CFTC's bearing capacity stipulated in regulatory instruments in a range of countries, e.g., Australia (Standard Australia AS5100.6-2004), Brazil (Brazilian Code NBR 8800:2008), Canada (CAN/CSA S16-01:2001), People's Republic of China (China Standard GB 50010-2010), Russia (CR 266.1325800.2016), and the USA (AINSI/AISC 360:2005), as well as the general European regulations (Eurocode EN 1994-1-1:2004), are essentially based upon empirical formulas. They have significant limitations in practical application, since they were obtained either from the results of specific laboratory sample tests (Furlong 1967; Tang et al. 1982; Saatcioglu and Razvi 1992; Shams and Saadeghvaziri 1997; Tsuda et al. 2000; Nishiyama et al. 2002; Johanson 2002; Fujimoto et al. 2004; Han 2007; Tao et al. 2008; Fattah 2012) or by the statistical processing of relevant data (Mander et al. 1988). First, these formulas are valid only for heavy concrete. For instance, in the case of the fine-grain concrete columns, they provide excessively high estimates. In compliance with the published results (Karpenko 1996), one can observe a significantly smaller gain in strength for fine-grain concrete under volumetric compression. When self-stressing concrete is used, such methods are not acceptable, as they do not take into account the pre-stress of the concrete core. Furthermore, empirical formulas are generally obtained by the results of research on small-scale samples, and their use often results in significant errors in the calculation of a bearing capacity for CFTCs with large cross-sections

*Correspondence: ep.chernyshova@gmail.com
[3] Department of Design, Institute of Civil Engineering, Architecture and Art, Nosov Magnitogorsk State Technical University, 11 Uritsky Str., Magnitogorsk 455000, Russia
Full list of author information is available at the end of the article
Journal information: ISSN 1976-0485 / eISSN 2234-1315

(500 mm and more). This is confirmed by the results of experiments on CFTCs having section diameters of 630–1020 mm (Fonov et al. 1989). In addition, these methods generally do not allow making consistent calculations of eccentrically compressed CFTCs when they have any differences from a "classical" design. Examples include the presence of a high-strength rod and (or) spiral reinforcement in a concrete core, which can be rather efficiently used in CFTCs. To calculate the stresses in such a reinforcement, if possible, it is necessary to obtain sample the axial and circumferential deformations. The known calculation methods for the strength of compressed CFTCs do not provide such an opportunity (Krishan et al. 2016).

Previous publications (De Oliveira et al. 2009; Dundu 2012) note that the most reliable results are given by the calculations of the CFTC strength performed on the basis of Eurocode 2 (EN 1992-1-1 2004). These norms suggest two approaches for calculations. The first approach is simplistic, based on empirical formulas, and acceptable when a number of simplifications are made. The general case of calculation is also considered. For this approach, it is necessary to take into account the geometric and physical nonlinearity of the structure and the processes of crack formation, concrete creep and shrinkage. However, these prescriptions are declarative in nature and are not supported by specific methods or formulas. At that, the indication of the necessity of deformation diagram use for volumetrically compressed concrete proposed in § 3.1.5 of EN 1992-1-1 is erroneous, as will be shown below.

Computer calculations also do not allow obtaining reliable results using finite element models (Hu et al. 2005; Liang and Fragomeni 2010). The software packages used for this purpose (ANSIS, ABAQUS, etc.) do not contain the possibility to change the transverse deformation ratio of concrete and steel as the voltage level increases. Without an appropriate modification in the form of a special subprogram, they do not allow the accurate determination of the magnitude of the concrete lateral pressure on a steel shell. This value determines the strength and deformation properties of the concrete and the ratio of the axial and circumferential stresses in the steel.

The purpose of this paper is to propose a calculation technique for the strength of short, non-centrically compressed CFTCs under short-term load action based on the phenomenological approach and the theoretical positions of reinforced concrete mechanics (Karpenko 1996).

2 Basic Design Provisions

Taking into account the design features of CFTCs, it is recommended to calculate their compressive strength on the basis of a nonlinear deformation model (Kotsovos 1980; Karpenko et al. 2013). The calculation is based on a number of assumptions. In particular, it is assumed that the cross-sections of the structure remain flat after their loading and that the joint operation of the steel and concrete components is ensured until CFTC destruction. The tensile strength of the concrete is not taken into account. To simplify the calculation, the residual stresses and geometric imperfections are replaced by equivalent initial flexural deviations, accounted for by random eccentricities. Consequently, the case of eccentric compression is always considered in the calculations. For compressed concrete-filled steel tube elements, the value of the random eccentricity is assumed to be no less than:

- 10 mm.
- $1/\Theta$,

where l is the length of the element or the distance between its sections fixed to prevent offsets and Θ is a coefficient that takes into account geometric imperfections along the length of the element, whose value is recommended to calculated by the following formula

$$\Theta = 500 - 50 \cdot \left(\rho_p^{0.25} + \rho_s^{0.5}\right), \tag{1}$$

in which ρ_p and ρ_s are the coefficients of the outer shell and longitudinal framework reinforcement, taken as percentages.

The calculation of the sample strength, performed using values of the concrete and steel strength characteristics obtained from the experimental results, should be carried out taking into account the understated values of random eccentricities. When samples are centred in the process of testing on a physical axis, this value is recommended to be reduced by 3 times.

The deformation calculation is based on material deformation diagrams. The CFTC power resistance is the work of the concrete and steel shell under the conditions of a volumetric stress state. As the loading level increases, the stress state changes not only quantitatively but also qualitatively. Therefore, the dependencies between the stresses and strains for concrete and steel are not known before the calculation begins. In this regard, the deformation calculation of the CFTC strength is proposed to be conducted in two stages.

In the first stage, diagrams of the concrete core $\langle\langle\sigma_{cz} - \varepsilon_{cz}\rangle\rangle$ and the steel shell $\langle\langle\sigma_{pz} - \varepsilon_{pz}\rangle\rangle$ are developed for the axial direction of the element. The diagram set is recommended to be of a multipoint form. It is shown (Karpenko et al. 2013) that this method is the most universal. In our case, it is practically realized during the calculation of the normal cross-section strength

of a short, centrally compressed CFTC, as is shown below.

In the second stage, using the known dependencies of the nonlinear deformation model, given, for example, in a set of rules (Krishan 2008), the strength of the centrally compressed CFTC is calculated.

2.1 Development of Material Deformation Diagrams

To develop the diagrams $\langle\langle\sigma_{cz} - \varepsilon_{cz}\rangle\rangle$ and $\langle\langle\sigma_{pz} - \varepsilon_{pz}\rangle\rangle$, the conditions for the joint operation of the concrete core and the steel shell are considered in the process of the incremental growth of the axial deformations $\varepsilon_{cz} = \varepsilon_{pz}$ of the centrally compressed column.

Concrete is represented by a transversely isotropic body that is under conditions of triaxial compression by axial stresses σ_{cz} and transversal stresses σ_{cr}. The form of the diagram is assumed to be curvilinear with a descending branch (Fig. 1).

The stress–strain state of the concrete can be analytically described on the basis of the dependences of the orthotropic model (Krishan 2008). The system of equations describing the relationship between the stresses σ_{cj} and deformations ε_{cj} for any point in the concrete is represented in the following form:

$$\begin{Bmatrix} \varepsilon_{cz} \\ \varepsilon_{cr} \end{Bmatrix} = \frac{1}{E_c} \times \begin{bmatrix} \nu_{cz}^{-1} & -2\upsilon_{zr}\nu_{ci}^{-1} \\ -\upsilon_{zr}\nu_{ci}^{-1} & (\nu_{cr}^{-1} - \upsilon_{rr}\nu_{ci}^{-1}) \end{bmatrix} \times \begin{Bmatrix} \sigma_{cz} \\ \sigma_{cr} \end{Bmatrix} \tag{2}$$

where E_c is the original elastic modulus of the concrete.

The consideration of the inelastic properties of the concrete core is made by the use of variable coefficients of elasticity ν_{cj} $(j = z, r, i)$ and transverse deformation $\upsilon_{zr}, \upsilon_{rr}$. Here, the indices z and r correspond to the axial and radial directions, and the index i corresponds to the elasticity coefficient, which determines the concrete deformation modulus in dependence between stress intensity and strain intensity.

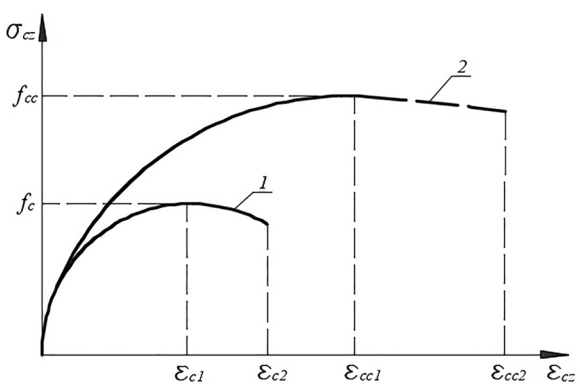

Fig. 1 Diagrams of concrete deformation under uniaxial compression (1) and with triaxial compression (2).

According to the values of the coefficients of elasticity ν_{ci} and transverse deformation υ_{zr}, υ_{rr} deformations along one (axial or transversal) direction are determined in the compliance matrix of the system (2), and these deformations are due to the stresses of the other direction (transverse or axial, respectively). These values depend on all the components of the complex stress–strain state of the concrete core, and therefore it is proposed to use the stress (σ_{ci}) and strain (ε_{ci}) intensity values to determine them. The values of the stress and deformation intensity are determined using the second invariants of the corresponding tensors. For a CFTC of a circular cross-section, the formulas for their calculation have a fairly simple form:

$$\sigma_{ci} = |\sigma_{cz} - \sigma_{cr}|; \tag{3}$$

$$\varepsilon_{ci} = \frac{2}{3}|\varepsilon_{cz} - \varepsilon_{cr}|. \tag{4}$$

The relationship between the intensities of the stresses and deformations is as follows:

$$\sigma_{ci} = \nu_{ci}E_c\varepsilon_{ci} \tag{5}$$

The values of the concrete transverse deformation coefficients increase with the compressive stress level from initial values $\upsilon_c = 0.18{-}0.25$ to extreme values $\upsilon_{jr} = \upsilon_{jru}$ $(j = z, r)$ at the top of the deformation diagram. It is suggested to calculate the coefficients υ_{jr} depending on the current ν_{ci}, the initial ν_{oj} and the extreme ν_{ciu} values of the concrete elasticity coefficient according to the formula:

$$\upsilon_{jr} = \upsilon_{jru} - (\upsilon_{jru} - \upsilon_c)\left(\frac{\nu_{ci} - \nu_{ciu}}{\nu_{oj} - \nu_{ciu}}\right)^{0.5}, \tag{6}$$

in which the extreme value of the transverse strain coefficient υ_{jru}, as well as the coefficients of elasticity, can be determined according to the recommendations of (Karpenko 1996).

The steel shell is represented as an isotropic body. The hypothesis of a single curve by Ilyushin is used to define it (Ilyushin 1948). According to this hypothesis, the connection between the stresses and deformations $\langle\langle\sigma_p - \varepsilon_p\rangle\rangle$, obtained with the uniaxial tension of a steel shell, is considered valid for all stressed states. Hence, the current stresses σ_p and deformations ε_p are replaced by the intensity of the current stresses σ_{pi} and the strain intensity ε_{pi}, respectively, for the sections of the shell under a complex stress state.

In numerous experiments, Chernov–Lüders lines with a slope of 45° to the longitudinal axis of the CFTC were

observed during the flow stage on the surface of the steel shell. Based on these data, the stresses and deformations arising at the main areas of the considered points of the steel shell are considered in the calculations, that is, the tangential stresses and shear strains are zero here. Then, the expressions for the intensities of the stresses and deformations have the following forms:

$$\sigma_{pi} = \frac{\sqrt{2}}{2}\sqrt{(\sigma_{pz} - \sigma_{p\tau})^2 + (\sigma_{p\tau} - \sigma_{pr})^2 + (\sigma_{pr} - \sigma_{pz})^2} \tag{7}$$

$$\varepsilon_{pi} = \frac{\sqrt{2}}{3}\sqrt{(\varepsilon_{pz} - \varepsilon_{p\tau})^2 + \left(\varepsilon_{p\tau} - \varepsilon_{pr}\right)^2 + \left(\varepsilon_{pr} - \varepsilon_{pz}\right)^2} \tag{8}$$

The initial diagram $\langle\langle \sigma_p - \varepsilon_p \rangle\rangle$ is recommended to be tri-linear (CR 266.1325800.2016 2016). However, when modelling steel sections under a complex stress state, it is advisable to use a deformation diagram calculated using the generalized parameters $\bar{\sigma}_{pi} = \sigma_{pi}/f_{yp}$ and $\bar{\varepsilon}_{pi} = \varepsilon_{pi}E_p/f_{yp}$ (Fig. 2), where f_{yp} and E_p are the yield strength and the elastic modulus of steel pipe, respectively. The coordinate values of the characteristic points of the generalized diagram can be taken from Table 1. The data of this table indicate that the transition from

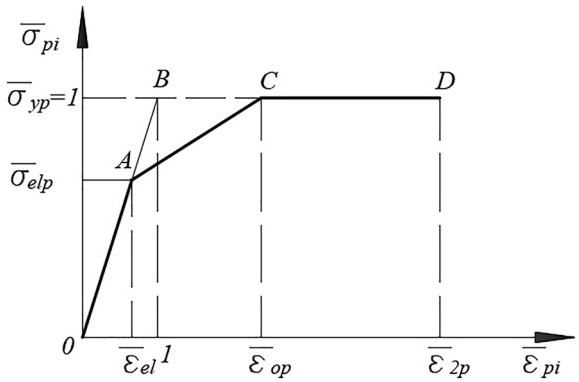

Fig. 2 Generalized calculation diagram of the steel shell operation.

the relative stresses $\bar{\sigma}_p$ to the relative stress intensity $\bar{\sigma}_{pi}$ increases the limit of the elastic work $\bar{\sigma}_{el}$. Thus, an original three-line diagram is upgraded to a two-line diagram for steels of C390 grade and higher.

The analytical relationship between the strains and stresses for any point of the outer steel shell in the elastic and elastic–plastic stages can be represented by the following system of equations:

$$\begin{Bmatrix} \varepsilon_{pz} \\ \varepsilon_{p\tau} \\ \varepsilon_{pr} \end{Bmatrix} = \frac{1}{\nu_p E_p} \times \begin{bmatrix} 1 & -\upsilon_p & -\upsilon_p \\ -\upsilon_p & 1 & -\upsilon_p \\ -\upsilon_p & -\upsilon_p & 1 \end{bmatrix} \times \begin{Bmatrix} \sigma_{pz} \\ \sigma_{p\tau} \\ \sigma_{pr} \end{Bmatrix} \tag{9}$$

Here, σ_{pz}, $\sigma_{p\tau}$, σ_{pr} are the normal stresses of a pipe in the axial, tangential and radial directions; ε_{pz}, $\varepsilon_{p\tau}$, ε_{pr} are the relative deformations of a steel shell in the corresponding directions; ν_p is the steel elasticity ratio; and υ_p is the coefficient of a steel pipe transverse deformation.

During the calculation of the CFTC strength, the stress–strain state of the concrete core and the steel shell is largely determined by the ratio of the concrete and steel transverse deformation current coefficients. That is why their precise definition is of fundamental importance. In Krishan et al. (2016), the value of the coefficient of transverse deformation for a steel shell υ_p is proposed to be determined by the formula:

$$\upsilon_p = 0.48 - (0.48 - \upsilon_0)\left(\frac{\nu_p - \nu_{pu}}{\nu_{po} - \nu_{pu}}\right), \tag{10}$$

in which ν_{po} and ν_{pu} are the coefficients of elasticity at the beginning of the deformation diagram and at the end of the yield point and υ_0 is Poisson's ratio for steel ($\upsilon_0 \approx 0.3$).

The values of υ_p calculated by the formula (10) are in good agreement with the data provided in the Russian Federation standards (Construction Rules and Regulations (CRaR) 2.05.06-85*), but calculations based on the

Table 1 Coordinates of diagram characteristic points of the steel shell deformation.

Diagram parameter	Steel grades according to CR 16.13330.2011					
	C245 C255	C285	C345 C345К C375	C390	C440	C590 C590К
$\overline{\varepsilon}_{el}$	0.80	0.80	0.80	0.90	0.90	0.90
$\overline{\sigma}_{elp}$	0.92	0.92	0.92	1.00	1.00	1.00
$\overline{\varepsilon}_{op}$	1.70	1.70	1.70	1.70	1.70	1.70
$\overline{\sigma}_{yp}$	1.00	1.00	1.00	1.00	1.00	1.00
$\overline{\varepsilon}_{2p}$	14.0	15.0	16.0	17.0	17.0	18.0

elastic coefficients make it possible to minimize the number of iterations.

In the elastic stage of the shell operation, when $\varepsilon_{pi} \le \varepsilon_{el}$, the value of the initial elasticity coefficient ν_{po} is determined according to the following formula:

$$\nu_{po} = \frac{\bar{\sigma}_{el}}{\bar{\varepsilon}_{el}}. \tag{11}$$

The following equation is used in the elastic–plastic stage when $\varepsilon_{el} \le \varepsilon_{pi} \le \varepsilon_{op}$:

$$\nu_p = \frac{\bar{\sigma}_{pi}}{\bar{\varepsilon}_{pi}}, \tag{12}$$

in which the relative intensity of the stresses $\bar{\sigma}_{pi}$ is determined by the following formula:

$$\bar{\sigma}_{pi} = \bar{\sigma}_{el} + \left(\bar{\sigma}_{yp} - \bar{\sigma}_{el}\right)\frac{\varepsilon_{pi} - \varepsilon_{el}}{\varepsilon_{op} - \varepsilon_{el}}. \tag{13}$$

The following dependence is used in a plastic stage:

$$\nu_p = \frac{\bar{\sigma}_{yp}}{\bar{\varepsilon}_{pi}}. \tag{14}$$

The following formula is obtained to calculate the lateral pressure on the concrete core from the solution of the systems of Eqs. (2) and (9), taking into account the equilibrium conditions and the joint deformation of concrete and steel:

$$\sigma_{cr} = \frac{\left(\upsilon_p - \beta_r \upsilon_{zr}\frac{\nu_{cz}}{\nu_{ci}}\right)\varepsilon_{cz}}{K_p + K_c} \tag{15}$$

in which $\beta_r = (d - 2\delta)/(d - \delta)$, and the expressions for K_p and K_c have the following form:

$$K_p = \frac{0.5\upsilon_p}{\nu_p E_{s,p}}\left[\upsilon_p\left(\frac{d}{\delta} - 1\right) - \left(\frac{d}{\delta} + 1\right)\right]; \tag{16}$$

$$K_c = \frac{\beta_r}{\nu_{ci}E_c}\left(\frac{2\upsilon_{zr}^2\nu_{cz}}{\nu_{ci}} + \upsilon_{rr} - \frac{\nu_{ci}}{\nu_{cr}}\right) \tag{17}$$

where d and δ are the outer diameter and the wall thickness of a steel pipe shell.

At a known value of σ_{cr}, the stresses in the steel shell $\sigma_{p\tau}$ and σ_{pr} are calculated. To do this, they consider the equilibrium condition for the cross section and use the Lame solution for the problem of stress determination in the walls of a thick-walled cylinder (Ilyushin 1948). Then, the stresses σ_{cz} are found from the first equation of the system (2), and the stresses σ_{pz} are found from the first equation of the system (9).

The limiting stress in the concrete $\sigma_{cz} = f_{cc}$ and the corresponding relative deformation of the concrete $\varepsilon_{cz} = \varepsilon_{cc1}$ (the coordinates of the curvilinear diagram vertex) are determined by the formulas obtained in Krishan 2008):

$$f_{cc} = \alpha_c f_c; \tag{18}$$

$$\varepsilon_{cc1} = \varepsilon_{c1}\alpha_c^{2.5}\left[1 - \frac{f_c}{\varepsilon_{c1}E_c}\left(1 - \alpha^{-1.5}\right)\right], \tag{19}$$

where f_c is the strength of the concrete under uniaxial compression; α_c is a coefficient that takes into account the increase in the concrete strength under triaxial compression; and ε_{c1} is the relative strain value of the shortening of uniaxially compressed concrete.

The coefficient α_c is calculated by the following formula:

$$\alpha_c = 0.5 + 0.75\bar{\sigma} + 0.25\sqrt{(\bar{\sigma} - 2)^2 + 16\bar{\sigma}/b}, \tag{20}$$

in which $\bar{\sigma}$ is the relative magnitude of the lateral pressure σ_{cr} from the steel shell side to the concrete core in the limiting state of the column $\bar{\sigma} = \sigma_{cr}/f_c$ and b is the material coefficient set on the basis of tests (for heavy concrete b = 0.096).

The relative value of the lateral pressure in the limiting state of the CFTC is found from the formula obtained in Krishan et al. (2016):

$$\bar{\sigma} = 0.4e^{-1.5b}\xi^{0.8}, \tag{21}$$

where ξ is the constructive coefficient calculated according to the following formula:

$$\xi = \frac{f_{yp}A_p}{f_c A}, \tag{22}$$

in which A and A_p are the cross-sectional areas of the concrete core and the steel shell, respectively.

The relative deformation of the concrete core under compression at the end of the stress-deformation diagram ε_{cc2} is determined with the help of a formula recommended by the norms of the Russian Federation (CR 266.1325800.2016 2016)

$$\varepsilon_{cc2} = \varepsilon_{c2}\frac{\varepsilon_{cc1}}{\varepsilon_{c1}}, \tag{23}$$

in which ε_{c2} is the relative deformation at the end of the diagram of uniaxially compressed concrete.

The analysis of formulas (18)–(20) shows that the values of both coordinates of the diagram top concerning the deformation of the concrete core largely depend on the magnitude of the concrete lateral pressure. In the process of the gradual increase of the axial deformation ε_{cz}, the pressure σ_{cr} does not remain constant. It increases from the values close to zero to a certain limiting value at $\varepsilon_{cz} = \varepsilon_{cc1}$ that depends on the constructive and geometric parameters of the CFTC and is determined by the means of formula (21). It is assumed

that at $\varepsilon_{cc1} \le \varepsilon_{cz} \le \varepsilon_{cc2}$, the lateral pressure does not change, i.e., $\sigma_{cr} = const$. Therefore, the value of stress in a concrete core at the deformation ε_{cc2} can be assumed as being equal to f_{cc}.

The result of this calculation is the entire family of diagrams $\langle\langle \sigma_{cz} - \varepsilon_{cz} \rangle\rangle$ (Fig. 3). It can be seen from the figure that at small deformation values ε_{cz}, the concrete core is in a state of uniaxial compression. For this state, formula (15) gives values $\sigma_{cr} \le 0$. Then, the stress σ_{cz} is determined according to diagram 1 (Fig. 3a, b). At certain values of ε_{cz}, a compressive lateral pressure appears on the concrete from the side of the steel shell. Then, the stresses σ_{cz} should be found from the deformation diagrams of the volume-compressed concrete with the lateral pressure σ_{cr} corresponding to each deformation.

Intermediate diagrams are used for a more accurate calculation of the elasticity coefficients, transverse strains and, ultimately, the stresses σ_{cz} corresponding to the accepted value of the deformation ε_{cz}.

Hence, it is obvious that it is impossible to use the deformation diagram of volumetrically compressed concrete in the limiting state recommended by Eurocode 4 (EN 1994-1-1 2004). In this case, the calculations give an increased bearing capacity, which is dangerous for practical use.

The practical implementation of the proposed calculation methodology is based on the step-iteration method. The axial deformation $\varepsilon_{cz} = \varepsilon_{pz}$ increases gradually, and at each step, the stress–strain state of the concrete core and the steel shell are calculated. It is then taken into account that the value of the relative deformation ε_{cc1}, originally calculated from formula (19), is only approximate, and it is specified during the calculation. Therefore, the iterations continue until the condition when the axial stresses in the concrete σ_{cz} reach its strength f_{cc} and the condition $\left|\varepsilon_{cc1}^{(k)} - \varepsilon_{cc1}^{(k-1)}\right| < \Delta_\varepsilon$ is fulfilled. In this condition k is the approximation number, and Δ_ε is the set accuracy of the calculations.

The result of this decision is arrays of numerical data that relate the relative deformations and stresses of the concrete and steel $\{\varepsilon_{czi}\}-\{\sigma_{czi}\}$ and $\{\varepsilon_{pzj}\}-\{\sigma_{pzj}\}$. They are then used to develop material deformation diagrams.

2.2 The Second Stage of the Calculation

During the second stage, using the obtained deformation diagrams, the bearing capacity of the non-centrally loaded CFTC is determined. The design scheme of the normal section of the concrete-filled steel tube element is shown in Fig. 4.

In general, a compressive force N_z with eccentricities e_x and e_y relative to the corresponding coordinate axes X and Y, as well as the bending moments M_x and M_y acting in planes XOZ and YOZ or parallel to them, are applied to the considered normal section of the element. These bending moments are defined by the formulas:

$$M_x = M_{xd} + N_z e_x; \tag{24}$$

$$M_y = M_{yd} + N_z e_y, \tag{25}$$

where M_{xd}, M_{yd} are the bending moments in the corresponding planes, determined from the static design calculation; N_z is the longitudinal force from an external load; and e_x and e_y are the distances from the point of the longitudinal force application to the corresponding coordinate axes.

With the direction of the axis n in the plane of the bending moment $M_n = \sqrt{M_x^2 + M_y^2}$, the case of compression by a force N_z applied with eccentricity $e_0 = M_n / N_z$ is regarded (see Fig. 4).

In the calculation process, the deformation of the most compressed fibre of the concrete core $\varepsilon_{c\max}$ is increased step by step. At each step, using the Bernoulli hypothesis, a diagram of the relative deformations of the normal cross section is designed, corresponding to the equilibrium condition of the calculated element. To develop such a diagram, it is necessary to find the corresponding value of the relative deformation of the least compressed (stretched) fibre of the steel shell $\varepsilon_{p\min}$. The search for this value is carried out with a gradual shortening deformation decrease (starting from $\varepsilon_{c\max}$) or a build-up of the elongation deformation $\varepsilon_{p\min}$ (starting from zero).

The normal section of the calculated element is conditionally divided into small sections with areas of concrete A_{ci} and steel shell A_{pk}. The origin of the coordinate system is combined with the geometric centre of an element cross-section.

Within each small section of the concrete core and the steel shell, the stresses are assumed to be uniformly distributed (averaged). The magnitude of the stresses is determined at the centre of gravity of each section, depending on the values of the corresponding deformations, using the results of the first stage of the calculation.

The equilibrium conditions, which are checked after each step of increasing the strain $\varepsilon_{c\max}$, are written as follows:

$$N_z = \sum_i \sigma_{czi} A_{ci} + \sum_k \sigma_{pzk} A_{pk}; \tag{26}$$

$$N_z e_0 = \sum_i \sigma_{czi} A_{ci} Z_{cni} + \sum_k \sigma_{pzk} A_{pk} Z_{pnk}, \tag{27}$$

in which Z_{cni} and σ_{czi} are the coordinates of the centre of gravity of the i-th section of the concrete and the stress in the axial direction at the level of its centre of gravity,

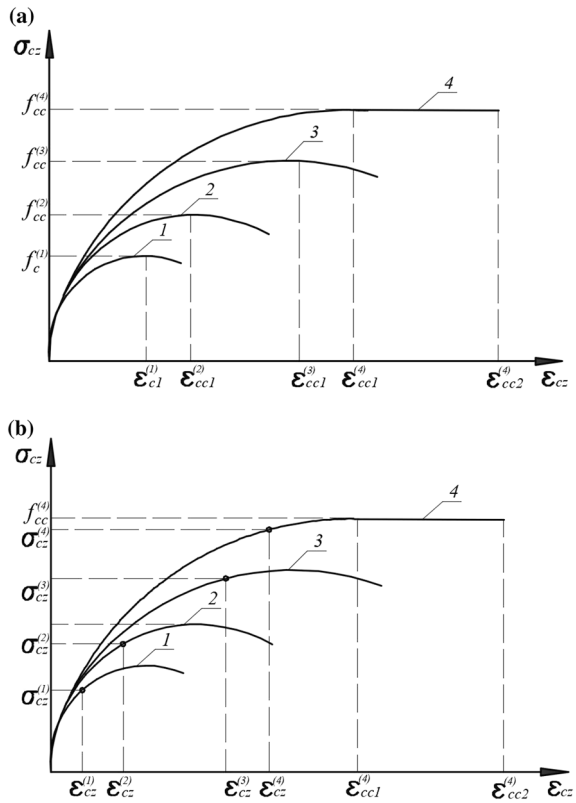

Fig. 3 The family of concrete deformation diagrams with a step-by-step increase of axial deformations: **a** the coordinates of diagram vertices, **b** to the determination of stresses with relative deformation increase; 1—uniaxial compression, 2, 3—volumetric compression at intermediate stages of deformation, 4—volumetric compression in the limiting state.

respectively, and Z_{pnk} and σ_{pzk} are the coordinates of the centre of gravity of the k-th section of the steel cage and the stress in the axial direction at the level of its centre of gravity.

When the equilibrium is reached according to the conditions (26) and (27), the value of the compressive force N_z corresponding to the set deformation ε_{cmax} is obtained. The relative deformations of the most compressed fibre of the concrete core are increased up to the limit value ε_{cu}, which is calculated according to the following formula:

$$\varepsilon_{cu} = 0.5\varepsilon_{cc2} + \sqrt{0.25\varepsilon_{cc2}^2 - (\varepsilon_{cc2} - \varepsilon_{cc1})\varepsilon_{cmin}}. \quad (28)$$

Then, $\varepsilon_{cmin} \leq 0$ (elongation deformation) should be taken as $\varepsilon_{cu} = \varepsilon_{cc2}$.

The problem of the bearing capacity determination is reduced to a search for relative deformation value of the shortening of the most compressed fibre $\varepsilon'_{cmax} \leq \varepsilon_{cu}$ corresponding to the maximum value of the compressive longitudinal force (Fig. 5). The results of the calculations in this formulation indicate that at certain structural parameters of the columns, the strength properties of the concrete core cannot be realized fully. Then, the normal stresses in the concrete do not reach its strength under triaxial compression. Such a design situation is sometimes encountered during the use of a strong steel shell with a sufficiently large ratio of the wall thickness to the diameter of the cross-section and relatively weak concrete. However, it is observed most often in columns of great flexibility, when the load-carrying capacity of the columns is determined by the loss of stability of the second type.

In this regard, the criterion for the loss of the load-carrying capacity of a column in the deformation calculation is the achievement of the maximum compressive force in the process of shortening the relative deformation increase of the most compressed fibre of a normal section.

On the other hand, in the process of a CFTC loading with certain geometric and constructive parameters, its axial deformation can reach excessively large values even before the exhaustion of the strength, and in such conditions, the operation of real structures becomes impossible. In a number of experiments, the axial deformations of CFTC samples reached 5–10%. In such cases, the limiting deformation can become predominant, determining the first limiting state. Therefore, during the determination of the CFTC load-bearing capacity, it is recommended to limit their axial deformations. The maximum permissible values of these deformations can be set by a calculator, depending on a specific design situation for a building or structure.

3 Comparison of Calculated Bearing Capacity with Experimental Data

In compliance with the proposed method, the authors developed an algorithm for the evaluation of the strain–stress state and the calculation of the bearing capacity of CFSTs having circular and annular sections. This algorithm is implemented in the software "CFST 3.3", registered with the Russian Agency for Patents and Trademarks (certificate of registration No. 2014614664). It provides an opportunity to calculate CFSTs made of heavy or fine-grain concrete (including self-stressing concrete) of classes from B15 up to B100 and a sheath made of any steel type, applied today, as well as to take into account the load duration and other norms for the manufacturing conditions and operation.

With the help of this software, the authors determined the theoretical values of the strength of CFTC short-compressed samples that were previously studied by the famous Russian scientific schools performing concrete-filled steel research (Fonov et al. 1989; Storozhenko et al. 1991). In addition, the experimental data of studies carried out at the Nosov Magnitogorsk State Technical

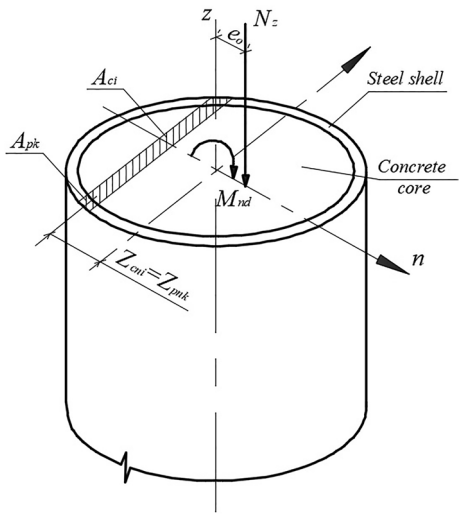

Fig. 4 Calculation scheme of the normal section CFTC.

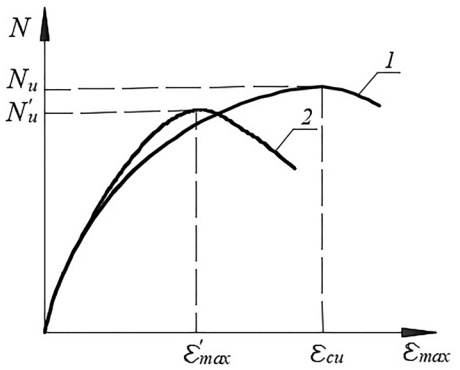

Fig. 5 Dependences of the compressive force from deformation of the most compressed fibre of concrete core: 1—with full implementation of strength properties of the concrete core; 2—for the cases when the strength properties of the concrete are not realized fully.

University in 2002–2017, both on columns with a prestressed concrete core and on conventional CFTCs (Krishan et al. 2016), are used.

CFTC samples of a circular cross-section, working under compression with random eccentricities (107 samples) and eccentric compression (60 samples), were considered. The relative eccentricity of the longitudinal force for the latter was in the interval $e_0/d = 0.06-0.375$. Some of the studied structures were made of self-stressing concrete. The conditions for carrying out all of the experiments and the obtained results are detailed in Krishan et al. (2016).

Table 2 provides a comparison of the obtained data with the experimental data of Japanese scientists (Nishiyama et al. 2002) who conducted large-scale and well-organized research on the considered problem. These results are of particular interest because they considered concrete and steel types of both low and high strength.

One should mention that to obtain unbiased information, the research considered the experimental data of samples with larger ranges of variation of the geometrical and design parameters:

- The outer diameter of the outer steel shell $-d=93-1020$ mm;
- The thickness of the outer steel shell wall $-\delta=0.8-13.3$ mm;
- The yield point of the shell steel $-f_{yp}=240-853$ MPa;
- The initial prismatic strength of the concrete $-f_c=11.7-104$ MPa.

The generalized results of the comparison are shown in Fig. 6. They indicate a completely satisfactory coincidence of the experimental destructive loads with the theoretical values. Concerning the samples subjected to compression with random eccentricities, the greatest discrepancies were $+19$ to -10%. The coefficient of the error vector variation, determined by the method of Eurocode 2 (EN 1992-1-1 2004), amounted to approximately $V_b=6\%$. For the eccentrically compressed samples, its value was approximately 8%. The inclination angle of the error vector in both cases is only slightly greater than 45°.

4 Discussion of Results

An analysis of these results indicates that the practical application of the developed calculation method gives a reliable and sufficiently stable estimate of the CFTC stress–strain state and strength. The nonlinear deformation model used as the basis of the method has significant advantages in comparison with the method of extreme forces. It allows one to use a single-system approach to the calculation of the bearing capacity and the stress–strain state of compressed concrete-filled steel tube elements at all stages of their operation. The practical implementation of this model is carried out using iterative calculation performed with the consideration of the complex stress state, as well as the inelastic deformations of the materials and the changes in the transverse deformation ratios in the core and the steel shell as the stress level rises. Such a calculation makes it possible to take into account the specifics of the compressed concrete-filled steel tube element operation.

The main dependencies for the determination of the strength and ultimate relative strain of triaxially compressed concrete were obtained phenomenologically on the basis of known positions in solid-body mechanics. Unlike the commonly used empirical formulas, they are

Table 2 Results of comparison of theoretical and empirical loads to failure.

No	Specimen ID	*d*, mm	*δ*, mm	f_{yp}, MPa	f_c, MPa	N_u^{Exp}, kN	N_u^{Th}, kN	N_u^{Exp}/N_u^{Th}
1	CC4-A-2	149	2.96	308	21.6	941	930	0.99
2	CC4-A-4-1	149	2.96	308	35.6	1064	1165	0.91
3	CC4-A-4-2	149	2.96	308	35.6	1080	1165	0.93
4	CC4-A-8	149	2.96	308	69.3	1781	1630	1.09
5	CC4-C-2	301	2.96	279	21.6	2382	2645	0.90
6	CC4-C-4-1	300	2.96	279	36.1	3277	3511	0.93
7	CC4-C-4-2	300	2.96	279	36.1	3152	3511	0.90
8	CC4-C-8	301	2.96	279	72.3	5540	5573	0.99
9	CC4-D-2	450	2.96	279	21.6	4415	5010	0.88
10	CC4-D-4-1	450	2.96	279	36.1	6870	6964	0.99
11	CC4-D-4-2	450	2.96	279	36.1	6985	6964	1.00
12	CC4-D-8	450	2.96	279	76.6	11,665	11691	0.99
13	CC6-A-2	122	4.54	576	21.6	1509	1211	1.24
14	CC6-A-4-1	122	4.54	576	35.6	1657	1450	1.14
15	CC6-A-4-2	122	4.54	576	35.6	1663	1450	1.15
16	CC6-A-8	122	4.54	576	69.3	2100	1890	1.11
17	CC6-C-2	239	4.54	507	21.6	3035	3026	1.00
18	CC6-C-4-1	238	4.54	507	35.6	3583	3818	0.94
19	CC6-C-4-2	238	4.54	507	35.6	3647	3818	0.95
20	CC6-C-8	238	4.54	507	69.3	5578	5210	1.07
21	CC6-D-2	361	4.54	525	21.6	5633	5700	0.99
22	CC6-D-4-1	361	4.54	525	36.1	7260	7300	0.99
23	CC6-D-4-2	360	4.54	525	36.1	7045	7300	0.99
24	CC6-D-8	360	4.54	525	76.6	11,505	10,812	1.06
25	CC8-A-2	108	6.47	853	21.6	2275	2131	1.07
26	CC8-A-4-1	109	6.47	853	35.6	2446	2254	1.09
27	CC8-A-4-2	108	6.47	853	35.6	2402	2250	1.07
28	CC8-A-8	108	6.47	853	69.3	2713	2618	1.04
29	CC8-C-2	222	6.47	843	21.6	4964	4389	1.02
30	CC8-C-4-1	222	6.47	843	35.6	5638	5207	1.08
31	CC8-C-4-2	222	6.47	843	35.6	5714	5207	1.10
32	CC8-C-8	222	6.47	843	69.3	7304	7346	0.99
33	CC8-D-2	337	6.47	823	21.6	8475	7765	1.09
34	CC8-D-4-1	337	6.47	823	36.1	9668	9929	0.97
35	CC8-D-4-2	337	6.47	823	36.1	9835	9929	0.99
36	CC8-D-8	337	6.47	823	76.6	13,776	13,971	0.99
Max		450	6.47	853	85.1	13,776	13,971	1.24
Min		108	2.96	279	25.4	941	930	0.88
V_b								0.085

more universal. In particular, they can be used for self-stressing, fine-grained and other types of concrete.

In addition, it should be noted that the developed method is applicable for the calculation of the bearing capacity both for traditional CFTCs and for those with pre-stressed concrete. The shape of the CFTC cross section and the nature of their reinforcement can thus be different. These differences are easily taken into account when calculation algorithms for specific problems are developed.

The proposed multi-point method for concrete deformation diagram development is of great importance for improving the calculation accuracy. So far, this diagram has been adopted either for uniaxially compressed concrete (without taking into account the effect of the cage) or for the volumetrically compressed concrete core of the structure under conditions of the limiting equilibrium. Thus, the value of the bearing capacity was underestimated in the first case and inflated in the second case. No new method had previously been developed.

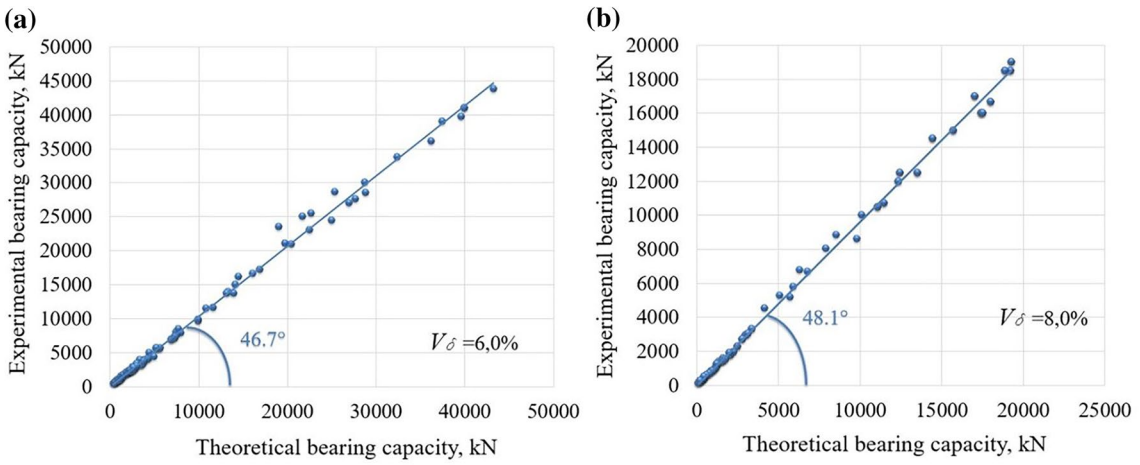

Fig. 6 Comparison of the bearing capacity theoretical values centrally (**a**) and eccentrically (**b**) compressed CFTC with experimental data.

The proposed criterion to achieve the load-carrying capacity of compressed elements is also important for practical calculations. It indicates that the strength properties of the concrete core cannot be used fully in certain cases. This fact cannot be ignored. In this regard, the calculation by the method of extreme forces does not always reflect the physical essence of the process and can result in large discrepancies from the experiments.

5 Conclusions

The authors proposed a method to determine the strength of short CFTCs. Based upon the known principles of a deformation calculation, it properly takes into account specific CFTC peculiarities. The method uses new dependencies to obtain the strength and ultimate deformation of a concrete core suitable for various concrete types, which makes it universal compared to other methods.

The deformation method of the strength calculation is based upon the numerical deformation diagram construction of a stressed concrete core and sheath. The implemented multipoint method of this diagram construction is significant for increasing the calculation accuracy.

The maximum value of a compression force is taken as a bearing capacity that is reached in the process of an incrementing relative deformation of shortening in the most compressed fibre with a normal section. This criterion allows a significant increase in the accuracy of the deformation calculation compared to the traditionally applied breaking stress method as allows a reliable assessment of the strain–stress state of compressed CFTCs.

Authors' contributions
ALK has developed the method to determining the strength of short CFTCs. MAA participated in the comparison of theoretical and experimental data of the work. EPC participated in the development of the method to determining the strength of short CFTCs and drafted the manuscript. All authors read and approved the final manuscript.

Author details
[1] Department of Building Design and Constructions, Institute of Civil Engineering, Architecture and Art, Nosov Magnitogorsk State Technical University, 11 Uritsky Str., Magnitogorsk 455000, Russia. [2] Institute of Civil Engineering, Architecture and Art, Nosov Magnitogorsk State Technical University, 11 Uritsky Str., Magnitogorsk 455000, Russia. [3] Department of Design, Institute of Civil Engineering, Architecture and Art, Nosov Magnitogorsk State Technical University, 11 Uritsky Str., Magnitogorsk 455000, Russia.

Acknowledgements
This article was prepared from the results of the implementation of a scientific project within the state task of the Ministry of Education and Science of the Russian Federation No. 7.3379.2017/4.6.

Competing interests
Not applicable.

Availability of data and materials
Not applicable.

Consent for publication
Not applicable.

Ethics approval and consent to participate
Not applicable.

Funding
Not applicable.

Publisher's Note

Received: 28 March 2018 Accepted: 24 November 2018
Published online: 29 December 2018

References

CR 266.1325800.2016. (2016). *Composite steel and concrete structures.* In *Design rules*. Ministry of Construction, Housing and Utilities of the Russian Federation.

De Oliveira, W. L. A., De Nardin, S., Debs, De Cresce El, de Cresce El, A. L., & El Debs, M. K. (2009). Influence of concrete strength and length/diameter on the axial capacity of CFT columns. *Journal of Constructional Steel Research, 65*(12), 2103–2110. https://doi.org/10.1016/j.jcsr.2009.07.004.

Dundu, M. (2012). Compressive strength of circular concrete filled steel tube columns. *Thin-Walled Structures, 56,* 62–70.

EN 1992-1-1. (2004). *Eurocode 2: Design of concrete structures*. Brussels: European Committee for Standardization.

EN 1994-1-1. (2004). *Eurocode 4: Design of composite steel and concrete structures*. Brussels: European Committee for Standardization.

Fattah, A. M. (2012). Behaviour of concrete columns under various confinement effects. Dissertation, USA, Kanzas: Kanzas State University.

Fonov, V. M., Lyudkovsky, I. G., & Nesterovich, A. P. (1989). The strength and the deformability of pipe-concrete elements under axial compression. *Concrete and reinforced concrete, 1,* 4–6.

Fujimoto, T., Mukai, A., Nishiyama, I., & Sakino, K. (2004). Behavior of eccentrically loaded concrete-filled steel tubular columns. *Journal of Structural Engineering, 130,* 203–212.

Furlong, R. W. (1967). Strength of steel encased concrete beam-columns. *Journal of the Structural Division, 93*(5), 115–130.

Han, L. H. (2007). *Concrete filled steel tubular structures* (2nd ed.). Beijing: China Science Press.

Hu, H. T., Huang, H. S., & Chen, Z. L. (2005). Finite element analyses of CFT columns subjected to an axial compressive force and bending moment in combination. *Journal of Constructional Steel Research, 61,* 1692–1712.

Ilyushin, A. A. (1948). *Plasticity*. Moscow: Gostekhizdat.

Johanson, M. (2002). The efficiency of passive confinement in CFT columns. *Steel Composite Structure, 2*(5), 457–464.

Karpenko, N. I. (1996). *General models of reinforced concrete mechanics*. Russia, Moscow: Stroyizdat.

Karpenko, N. I., Karpenko, S. N., Petrov, A. N., & Palyuvina, S. N. (2013). *Model of reinforced concrete deformation in increments and the calculation of beams-walls and bent plates with cracks*. Petrozavodsk: Publishing house of PetrSU.

Kotsovos, M. D. (1980). A mathematical model of the deformational behavior of concrete under generalized stresses based on fundamental material properties. *Journal of Construction Materials, 13,* 289–298.

Krishan, A. L. (2008). New approach to estimating the durability of compressed pipe-concrete columns. In *Concrete durability: Achievement and enhancement: Proceedings of the 7th international congress*, Scotland: University of Dundee, 8-10 July 2008 (pp. 143–151).

Krishan, A. L., Astaf'eva, M. A., & Sabirov, R. R. (2016). *Calculation and construction of concrete filled steel tube columns*. Saarbrucken: Palmarium Academic Publishing.

Liang, Q. Q., & Fragomeni, S. S. (2010). Nonlinear analysis of circular concrete-filled steel tubular short columns under eccentric loading. *Journal of Constructional Steel Research, 66*(2), 159–169.

Mander, J. B., Priestley, M. J. N., & Park, R. (1988). Theoretical stress-strain model for confined concrete. *Journal of Structural Engineering, ASCE, 114*(8), 1804–1826.

Nishiyama, I., Morino, S., Sakino, K., & Nakahara, H. (2002). *Summary of Research on Concrete-Filled Structural Steel Tube Column System Carried Out Under The US-JAPAN Cooperative Research Program on Composite and Hybrid Structures*. Japan.

Saatcioglu, M., & Razvi, S. R. (1992). Strength and ductility of confined concrete. *Journal of Structural Engineering, 118*(6), 1590–1607.

Shams, M., & Saadeghvaziri, M. A. (1997). State of the art of concrete-filled steel tubular columns. *ACI Structural Journal, 94*(5), 558–571.

Storozhenko, L. I., Plakhotny, P. I., & Cherny, A. Ya. (1991). *Calculation of concrete filled steel tube structures*. Kiev: Budivelnik.

Tang, C., Zhao, B., Zhu, H., & Shen, X. (1982). Study on the fundamental structural behavior of concrete filled steel tubular columns. *Journal of Building Structures, 3*(1), 13–31.

Tao, Z., Uy, B., Han, L. H., & He, H. S. (2008). Design of concrete-filled steel tubular members according to the Australian Standard AS 5100 model and calibration. *Australian Journal of Structural Engineering, 8*(3), 197–214.

Tsuda, K., Matsui, C., & Fujinaga, T. (2000). Simplified Design Formula of Slender Concrete-Filled Steel Tubular Beam-Columns. In *Proceedings of the 6th ASCCS conference on composite and hybrid structures*, Los Angeles, 1 (pp. 379-396).